POAC'13
Espoo, Finland

Proceedings of the 22nd International Conference on
Port and Ocean Engineering under Arctic Conditions
June 9-13, 2013
Espoo, Finland

Frequency domain force identification in ice-structure interaction

Torodd S. Nord [1], Mauri Määttänen [2], Ole Øiseth [3]

[1, 2)] Sustainable Arctic Marine and Coastal Technology (SAMCoT), Centre for Research-based Innovation (CRI), Norwegian University of Science and Technology, Trondheim, Norway

[3] Norwegian University of Science and Technology (NTNU)/ Department of Structural Engineering, Trondheim, Norway.

ABSTRACT

A deterministic force identification method has been applied in ice-structure interaction. A compliant structure was forced through ice sheets in laboratory (EU-HYDRALAB DIIV test campaign at HSVA in 2011). Structural vibrations caused by crushing failure occurred over a range of velocities and frequencies. The experimentally obtained frequency response function (FRF) matrices and the measured responses were used to solve the inverse problem of identifying the forces at the ice action level.

The forces from two vibration tests are presented together with parametric Burg spectra of the responses. They indicate that forces drop on the transition between vibration frequencies, while maximum forces occur with presence of two dominating frequencies. No clear relationship between the natural frequencies, measured response and the peak forces was found.

INTRODUCTION

Pressure panels, tactile sensors and load cells are some of the direct measurement techniques which can estimate the loads on structures in different scales. Frederking et al. (2002) present a thorough review of load panels installed on the Molikpaq platform, after being deployed offshore Sakhalin. The evaluation of system performance and improvements suggested to enhance the ability to operate in arctic conditions provide a valuable insight to the challenges met in full-scale experimental testing.

The tactile sensors/panel sensors have been used in ice research by Takeuchi et al. (2000), Sodhi (2001), Taylor (2009), Määttänen et al. (2011) and Hendrikse et al. (2012). These sensors have the advantage that they can measure pressure with a high spatial resolution. They can be tailored to fit the indentor and enable extraction of both contact area and pressure. However, the sensors can only measure normal forces/stresses so that any shear forces/stresses have to be derived through assumed static and dynamic friction coefficients. When the stresses exceed elastic domain and material softening may be present, assuming a shear distribution becomes even more challenging.

The ice load survey carried out by Timco and Croasdale (2006) shows that there is considerable uncertainty, even within the ice research community, in prediction of ice loads on structures. Laboratory experiments are one of the ways that we can control to some extent both structure and ice conditions, aiming to adapt the knowledge into full scale. Different

laboratory studies on compliant structures (E.g. Määttänen (Määttänen, 1978; Määttänen, 1983; Määttänen et al., 2012), Kärnä (Kärnä, 1995; Kärnä et al., 2003), Toyama et al. (1983), Sodhi (2001) ,Gravesen et al. (2005) and Barker et al. (2005)) use different tehniques and measurement setups to derive the ice-forces. Many of the test-setups use direct measurement of the global ice force with load cells and dynamometers while others use indirect calculation of forces from structural response. The dynamometers give easy access to forces, still the added mass from water and model mass have to be dealt with. Load cells built into the indentor together with an accelerometer is possible in laboratory, but scarcely applicable on full-scale offshore structures.

Inverse force identification is a research topic adopted into structural dynamics and applied on systems where the forces are difficult to measure directly. For civil engineering purposes, bridges, piers, lighthouses and offshore structures interacting with ice are all examples where the ice force is difficult to quantify. The thesis by Lourens (2012) summarizes and qualitatively assess different linear approaches, while Kerschen et al. (2006) take the step further with a survey through nonlinear system identification methods. The classical book by Ewins (2000) explains vibratory experimental testing thoroughly, from the development of frequency response matrices to force identification. The frequency domain method was investigated by Fabumni (1986), who evaluated the effect of erroneous response signals, FRF matrix and number of forces to be identified. A general approach to establish a force-prediction model in the frequency domain is proposed by Wang (2002), who suggest an update of the analytical FRF from the measured response. Parloo et al. (2003) extend the framework to identify forces when the FRF matrix is not measurable anymore, which could be the scenario in ice-structure interaction.

In ice, the so far work on inverse force identification is limited, and restricted to deterministic frequency domain methods. Määttänen ((1983) ,(1982)) Singh et al. (1990), Timco et al. (1989) and Montgomery and Lipsett (1981) utilized the inverse force identification technique. Singh et al. (1990) emphasise the problems with what they refer to as a transfer function approach, and achieve interesting results by increasing the damping in the transfer function towards the damping observed during ice crushing in laboratory. Montgomery and Lipsett (1981) applied inverse force identification in full scale experiments. Accelerometers attached to bridge piers were set to measure the response during ice action and forces were solved inversely in the frequency domain.

The aim for this paper is to identify the ice force at different velocities acting on a compliant structure, solved in the frequency domain from measured responses. The force is solved solely based on measured FRF matrices in ice-free conditions, not modified with updated damping coefficients or added mass. The forces are sought at a location where no sensors measuring response are deployed, hence this is a so-called *non-collocated* problem (Nordström and Nordberg, 2004). A pseudo-inverse technique is used to invert the non-square FRF matrix, thus a least square solution of the forces is obtained. The response frequency components are presented in a Burg spectrum. That presentation enables direct comparison between forces and time-variant response frequency components. The attributes to both forces and measured responses are discussed and compared with the velocities and ice properties.

FORCE IDENTIFICATION IN THE FREQUENCY DOMAIN

The frequency domain deconvolution method belongs to the class of deterministic methods. Only a brief review of the method is presented here, but further details can be found in Ewins

(2000). For a single degree of freedom system, the dynamic response can be obtained by the following convolution integral in time domain:

$$u(t) = \int_0^t h(t-\tau)p(\tau)d\tau \tag{1}$$

Here, u(t) and p(τ) represent the response and the dynamic action respectively, while $h(t)$ is the response function for a unit impulse excitation. By applying the Fourier transform to the convolution integral in Eq.(1), the relation between response and applied excitation becomes:

$$\hat{u}(\omega) = \hat{H}(\omega)\hat{p}(\omega) \tag{2}$$

where $\hat{H}(\omega)$ is the complex frequency response function (FRF) of a system exited by a unit harmonic impulse. For multiple degree of freedom systems, the output $\hat{u}_i$ is a vector of n^d measured responses and $\hat{p}_j$ a vector of n^p unknown forces, hence we obtain the following system:

$$\hat{\mathbf{u}}(\omega)_{n^d \times 1} = \hat{\mathbf{H}}(\omega)_{n^d \times n^p}\hat{\mathbf{p}}(\omega)_{n^p \times 1} \tag{3}$$

The elements in the FRF matrix $\hat{H}_{ij}$ represents the response at a specific location *i* from an applied load at location *j*. It can either be determined experimentally or obtained numerically. If $n^d = n^p$, the FRF matrix is of full rank and the inverse problem can be solved by pre-multiplying Eq.(3) by $(\hat{H}_{ij})^{-1}$. In most cases, $n^d > n^p$, and use of an pseudo-inverse technique is necessary in order to solve the system. The pseudo-inverse of the non-square FRF matrix can be written in the following form:

$$\hat{\mathbf{H}}^{\dagger} = (\hat{\mathbf{H}}^H\hat{\mathbf{H}})^{-1}\hat{\mathbf{H}}^H, \tag{4}$$

where *H* is referring to the Hermitian transpose. The input forces are identified from the measured output responses and the pseudo-inverse of the FRF matrix:

$$\hat{\mathbf{p}}(\omega)_{n^p \times 1} = \hat{\mathbf{H}}^{\dagger}(\omega)_{n^d \times n^p}\hat{\mathbf{u}}(\omega)_{n^d \times 1} \tag{5}$$

After the complex forces $\hat{\mathbf{p}}(\omega)_{n^p \times 1}$ are identified, an inverse fast Fourier transform (FFT) can be applied to convert the forces into time domain.

EXPERIMENTAL SETUP

Structural properties

The identification method is applied on analysis of data from the *Deciphering Ice Induced vibration* (EU-HYDRALAB DIIV) test campaign at HSVA in 2011 (Määttänen et al. (2012), Hendrikse et al.(2012), Nord and Määttänen (2012)). A beam supported by horizontal leaf springs and vertical supports was constructed to vibrate with two dominant modes in the frequency range of interest. A cylindrical indentor with 220mm diameter was installed to the main beam at the ice action level. Figure 1 shows the set-up where the test structure is fixed to a 50 tonne carriage that drives with a predefined velocity (Figure 4, bottom row) through the ice-sheets while measuring responses. A set of different ice-thicknesses, temperatures and structural configurations (mass and stiffness adjustable) provided a range of comparable data-sets.

Data acquisition

Four response measurements were used firstly, to identify the FRF matrix and secondly to identify the force at the ice action level. Two lasers and two strain gauges were installed to measure the responses at locations on the lower part of the structure as shown in Figure 1. The sampling rate of 100Hz was applied to all channels, both during dynamic calibration and ice

action. The load cell was only used during the free vibration test to estimate the FRF matrix, thereby not used during ice interaction.

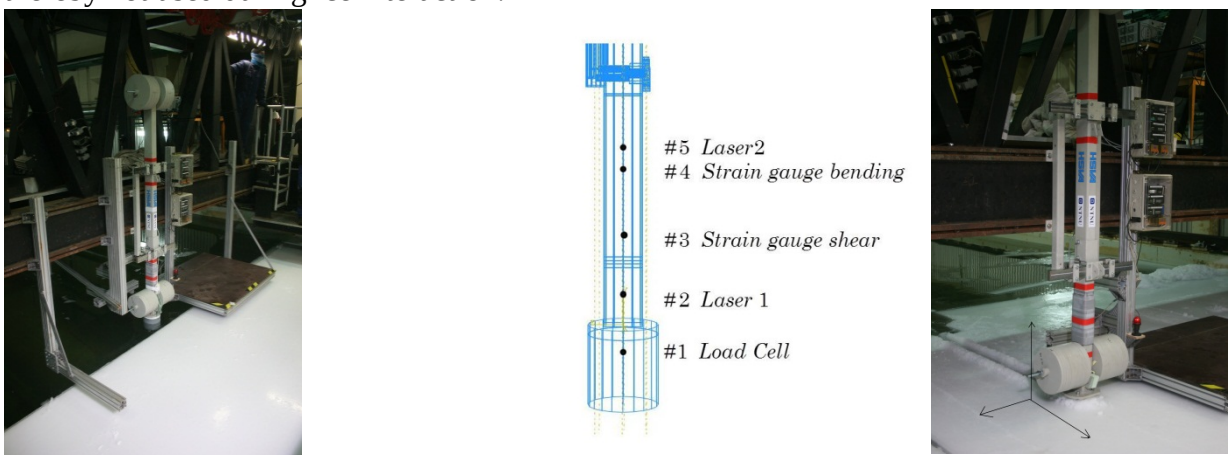

Figure 1. Test structure and sensor locations.

Ice properties

The ice sheets were homogeneous and columnar structured. Initial seeding and scraping the ice sheets from underneath controlled the grain size. Test 3300 had relatively warm ice, hence the compressive and flexural strength were low. Colder and thicker ice was present for the 4300 test, while the grain size was kept on similar level. A summary of the properties used in both tests is given in Table 1.

Table 1. Test setup properties.

Property	Test 3300	Test 4300	Property	Test 3300	Test 4300
Ice thickness, h_{ice} mm	58	60	Salinity, S ppt	3.2	3.2
Ice density, ρ kg/m^3	836.1	829.7	Indentor width,w mm	220	220
Flexural strength, σ_f N/mm^2	0.099	0.164	Aspect ratio, w/h_{ice}	3.79	3.67
Compr. Strength, σ_c N/mm^2	0.167	0.393	1st Nat. Frequency, f_1 Hz	10.2	12.2
Ice Temperature, T_{ice} ^{o}C	-0.8	-1.7	2nd Nat. Frequency, f_2 Hz	15.4	16.2

EXPERIMENTAL RESULTS

Experimentally determination of FRF matrix

In order to identify the ice actions, the FRF matrix of the system is needed. A survey of methods to determine the FRF matrix and their limitations have been thoroughly described by Ewins (2000). A step relaxation test in open water was chosen for the dynamic calibration. The response and applied load were measured when a steel rod connected to the ice action point was gradually loaded. In between the rod and the ice-action point there was a weak-link installed which went to failure with a certain applied load, typically 10kN. The FRF matrix elements can be determined from the applied load and measured response in the frequency domain:

$$\hat{H}_{ij}(\omega) = \frac{u_i(\omega)}{p_j(\omega)}, \tag{6}$$

where the complex $u_i(\omega)$ and $p_j(\omega)$ were determined by taking the fast Fourier transform (FFT) of the responses, $u_i(t)$, and applied excitations, $p_j(t)$. As outlined in Figure 1, four non-collocated responses were measured in DOF *i=2..5*. Element $\hat{H}_{11}$ is unknown since no measured response is available at the ice action point. Because of the missing measurement

DOF's, the FRF matrix is truncated. The real and imaginary parts of element $\hat{H}_{41}$ in the experimentally obtained FRF matrix are displayed in Figure 2. As expected, there are two frequencies that dominate the response, in this case about 12 and 16Hz. For every structural configuration, dynamic calibrations were performed such that the FRF could be obtained experimentally. All structural configurations were also compared with 3D FEM models for verification, see Nord and Määttänen (2012) for further details.

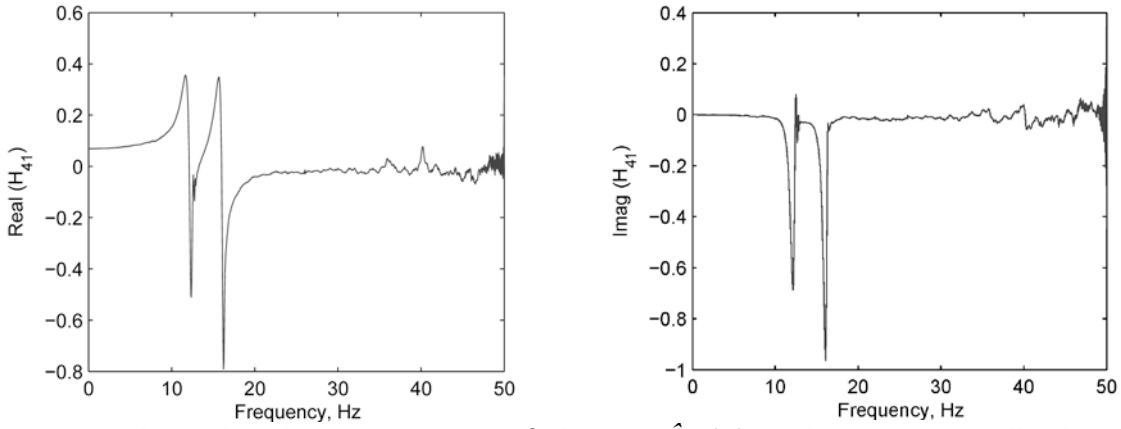

Figure 2. The real and imaginary part of element $\hat{H}_{41}(\omega)$ in the experimentally determined frequency response matrix.

Force identification

The forces were identified according to Eq. (5), with ¾ overlapping time segments of 2048 points. A statistical presentation of the forces is chosen to simplify the comparison between forces, responses and velocities. The data are processed by dividing the test series lengths into N=60 time intervals from $t_1 \ldots t_N$ illustrated in Figure 3. For every 2048pt force window that is identified, the forces are sorted into the corresponding time interval. The same procedure is used on the recorded carriage velocity (ice-sheet velocity). In each time interval, the mean (F_{av}), standard deviation (F_{std}) and peak forces are found. A threshold for selecting the peak forces is set equal to the mean value, and F_{maxav} denotes the average of the peak forces above this threshold value. The total length T for the analysed test-series 4300 and 3300 is chosen to be equal. However, the time before the structure hit the ice-edge is left out, which causes different lengths of the two time axes (Figure 4). The analysed data in this paper exclude most of the intermittent crushing, leaving the discussion to the continuous brittle crushing regime.

The forces, corresponding strain gauge responses and carriage velocities are shown in the upper, mid and bottom row of Figure 4, respectively. By comparison of the forces and the velocity intervals in test 4300, a repeated pattern can be observed in both the mean values, F_{av} and maximum values, F_{maxav} . Next to each velocity shift, the forces increase until they reach a local maximum. Thereafter the forces decrease until the transition to the next velocity interval. At the time when the global maximum occurs (t=270s, v=100mm/s), two dominating frequencies appear in the response spectrum. Subsequent response characteristics change both in number of active frequencies and their respective values. The forces decrease significantly when only one response frequency is present. The reductions are 25% and 24% in F_{av} and F_{maxav} respectively, calculated from the peak (t=270s) until the last interval (t=290s). Weaker and thinner ice in test 3300 explains the low forces. Two active frequency components are present at the instant of the global force maximum (t~108s). As seen from Figure 4, the velocity at that point is slightly above (v=180mm/s) the previous test. The force reductions

are now 28% and 32%, representing F_{av} and F_{maxav} respectively. These reductions depend on the point to represent the force after the decrease, selected to t=134s in this test.

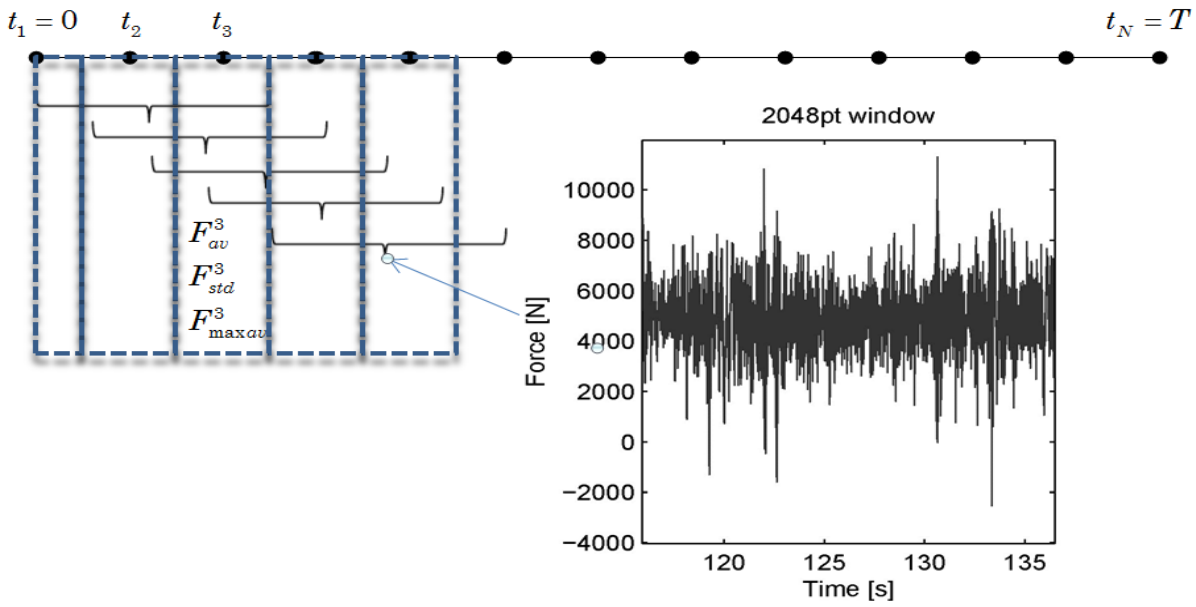

Figure 3. Post-processing routine for the identified forces.

Structural Response

The ice velocity was increased with time during both tests as displayed in Figure 4**.** In test 4300 the velocity was increased in steps, while a constant acceleration was applied in test 3300. At low velocities (v<80mm/s) in test 4300, the ice followed the deflection of the structure with ductile load build up, and the spring-back effect with brittle failure. This intermittent crushing event was only present for a few seconds before continuous brittle crushing dominated the failure process. Both tests had relatively warm ice, hence the ice was weak as seen from the measured compressive and flexural strength values in Table 1. Underwater-cameras revealed that the extrusion of crushed ice primarily consisted of small particles with some larger pieces spalling off. Radial cracks were occasionally observed, but they did not expand to the walls of the ice tank.

A Burg parametric filter was used to create the spectra of the strain gauge response signals. The response spectra of both tests are shown in the mid row of Figure 4, plotted with logarithmic scale pointing perpendicular to the plane. Horizontal red lines are added to the figures to represent the natural frequencies from open water calibration.

The analysed time-sequence in test 3300 covers the velocities between 70mm/s and 260mm/s. The red bands changing with time in the response spectra represent the presence of significant frequency components. While the dominating frequency components appear somewhat below the first and second natural frequencies at t<100s, respectively, they dislocate towards higher frequencies for t>100s. The highest frequency component crosses the second natural frequency as time exceeds 100s, while the lowest component occurs still below the first natural frequency. The frequency components seem to stabilize and the red bands in Figure 4 are kept almost constant prior to a second frequency shift at t~120s. After 120s, the energy in the second frequency component is gradually lost and subsequent crushing occurs with

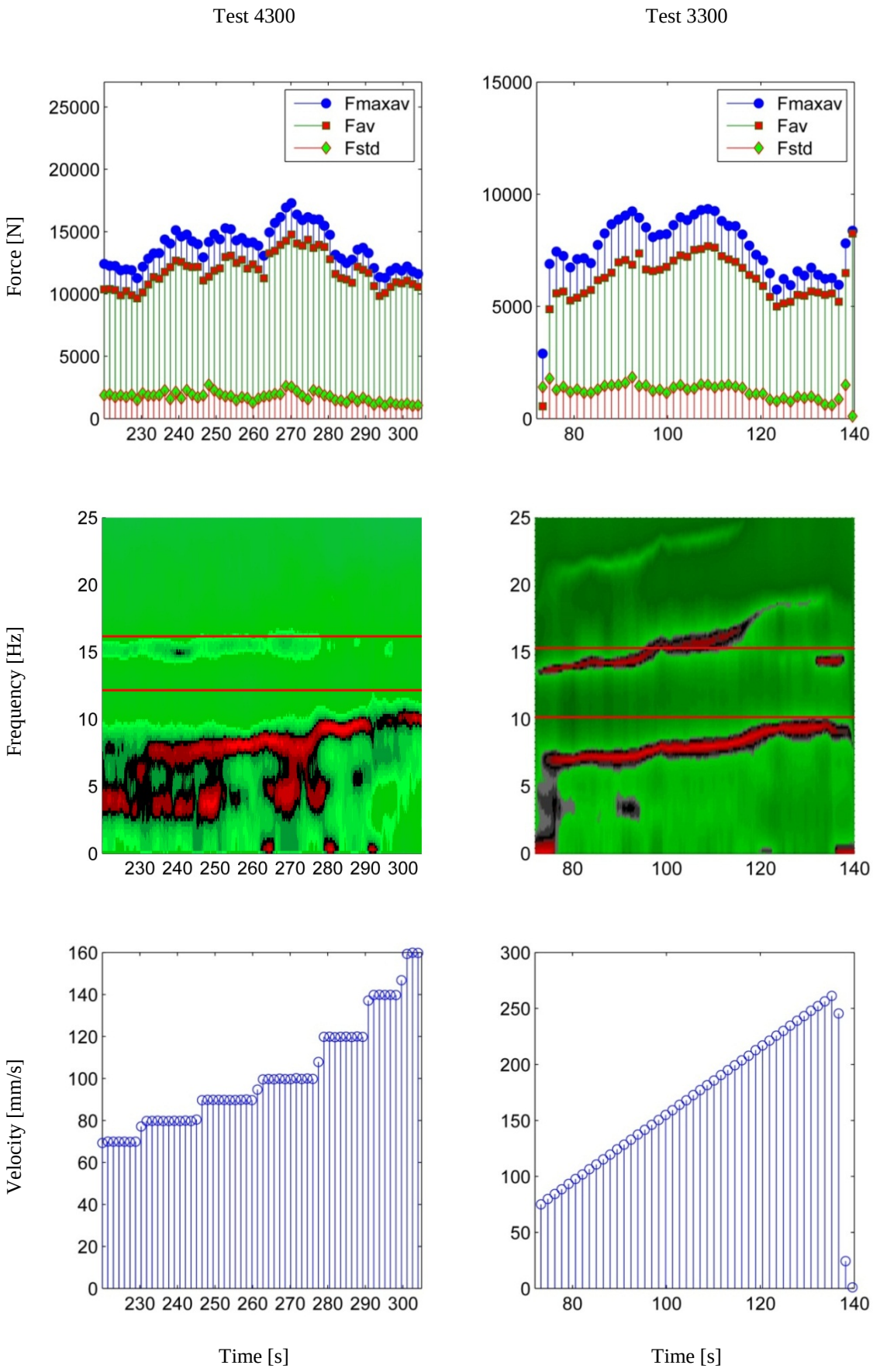

Figure 4. Top row: Identified forces. Mid row: Response spectra (Red color: High energy, green color: low energy) . Bottom row: Ice (carriage) velocity.

primarily one single vibration frequency close to the first natural frequency. Thereafter the carriage brakes down to zero velocity, hence the zero frequency component increases.

The significant response frequencies in test 4300 increased with time as the velocity increased for each interval. Evidently the response is not controlled in a single narrow band, but with smaller contributions spread at different frequencies. Still, the major vibration frequencies are possible to address in the spectrum. Minor contributions between 2-4Hz are recognized, and possibly related to that intermittent crushing occasionally controlled the interaction process. During the test, both the number of active frequencies and their content appear prone to velocity changes. At the time when the velocity shifts are doubled in magnitude (v>100mm/s) the frequency components displace more than what we observe at low velocity levels (v<100mm/s) when the velocity shifts were less.

DISCUSSION

Correlation of forces with response and ice properties

Apparently the intervals with constant velocities (4300) and constant acceleration (3300) have their distinct characteristics. The local force maxima occurred only for constant velocities. As the constant acceleration is low (~3mm/s^2), these rapid changes are not likely to occur, thus no local effects are identified for this configuration.

The low velocities in test 4300 may explain the low frequency contents (2-4Hz) to originate from the domain of intermittent crushing. At the time when the maximum force occurs, the two frequency components are both below the first natural frequency. For test 3300, the components below 5Hz are negligible and the frequency band close to the second natural frequency appears more dominant. Still, two frequency components located below each natural frequency are active at the time when the force reaches the maximum.

The results indicate that forces change both with the number of dominant vibration frequencies and their representative values. Despite that no force spectra are presented in this paper, both tests indicate that when the number of active frequencies is reduced from two to one, the forces decrease significantly. Noticeable the forces drop in the vicinity of a sudden frequency shift. It is not achieved to identify if the shift can be regarded as a change in the dynamic system. The identified dynamic component F_{maxav} appears low compared with F_{av}, whereas the study of Määttänen (1983) showed a more prominent dynamic contribution. The standard deviations of the forces, F_{std}, tend to decrease towards the end of both tests, implying a lower dynamic contribution in the forces at high velocities. The strikingly low dynamic force components may originate from the characteristics of the ice. Viscous behaviour of the ice could cause the material ahead of the indentor to dissipate more energy in the extrusion phase, causing additional damping of the vibration amplitudes.

Identification method

The classical paper by Fabumni (1986) explores the limitations by this method when random error is added to the response signal and the mobility matrix. Despite 15% random error introduced in the mobility matrix, one force could be determined on a cantilever beam with good accuracy. The number of forces, non-collocation of measurement sensors and the error are of importance, but also the general assumption that the forces can be identified from the experimentally obtained FRF without presence of ice. In the vicinity of the natural frequencies it is difficult to predict forces; however, the examples of forces given in this paper show those regions where the response is far from the natural frequencies. A paper by Hollandsworth (1989) demonstrates the effect of the non-collocation of the sensors, which

causes an underestimation of the applied forces. Hence the low maximum force level may not solely be explained by ice-properties, but also connected to the non-collocation of the sensors.

The discussion regarding which dynamic regimes the forces can be trusted has met low attention in ice-research besides the papers mentioned in the introduction. More sophisticated identification methods may bring new answers into the topic, whereas the research so far has been limited to the deterministic frequency domain methods.

CONCLUSION

In this work, the ice forces acting on a flexible structure were identified from experimentally obtained FRF matrices and measured responses from a set of non-collocated measurement transducers. The identified ice forces change with the number of active response frequencies and the corresponding frequency contents. The force maximum in both tests occurred when the responses had more than one major frequency component active.

ACKNOWLEDGEMENT

The authors wish to acknowledge the support from the Research Council of Norway through the Centre for Research-based Innovation SAMCoT and the support from all SAMCoT partners. The work described in this paper was supported by the European Community's 7th Framework Programme through the grant to the budget of the Integrated Infrastructure Initiative HYDRALAB-IV, Contract no. 261520. The authors would like to thank the Hamburg Ship Model Basin (HSVA), especially the ice tank crew, for the hospitality, technical and scientific support and the professional execution of the test programme in the Research Infrastructure ARCTECLAB.

REFERENCES

Barker, A., Timco, G., Gravesen, H. and Vølund, P., 2005. Ice loading on Danish wind turbines: Part 1: Dynamic model tests. Cold Regions Science and Technology, 41(1): 1-23.

Ewins, D.J., 2000. Modal Testing: Theory, Practice and Application, Second Edition.

Fabumni, J.A., 1986. Effects of structural modes on vibratory force determination by the pseudoinverse technique. AIAA Journal, 24(3): 504-509.

Frederking, R., D.Masterson, B.Wright and Spencer, P., 2002. ICE LOAD MEASURING PANELS – THE NEXT GENERATION, IAHR, New Zealand, pp. 450-457.

Gravesen, H., Sørensen, S.L., Vølund, P., Barker, A. and Timco, G., 2005. Ice loading on Danish wind turbines: Part 2. Analyses of dynamic model test results. Cold Regions Science and Technology, 41(1): 25-47.

Hendrikse, H., Metrikine, A. and Evers, K.-U., 2012. A method to measure the added mass and added damping in dynamic ice-structure interaction:, "Ice Research for a Sustainable Environment"(IAHR). Dalian, China.

Hollandsworth, P.E. and Busby, H.R., 1989. Impact force identification using the general inverse technique. International Journal of Impact Engineering, 8(4): 315-322.

Kerschen, G., Worden, K., Vakakis, A.F. and Golinval, J.-C., 2006. Past, present and future of nonlinear system identification in structural dynamics. Mechanical Systems and Signal Processing, 20(3): 505-592.

Kärnä, T., 1995. Finite ice failure depth in penetration of a vertical indentor into an ice edge : T. Karna, Annals of Glaciology, 19, 1994, pp 114–120. International Journal of Rock Mechanics and Mining Sciences & Geomechanics Abstracts, 32(2): A98.

Kärnä, T., Kolari, K., Jochmann, P., Evers, K.-U., Xiangjun, B., Määttänen, M. and Martonen, P., 2003. Ice action on compliant structures, VTT research notes 2223, VTT.

Lourens, E.-M., 2012. FORCE IDENTIFICATION IN STRUCTURAL DYNAMICS. PhD Thesis, Katholieke Universiteit Leuven.
Montgomery, C.J. and Lipsett, A.W., 1981. ESTIMATION OF ICE FORCES FROM DYNAMIC RESPONSE, International Symposium on Ice (IAHR), Quebec, P.Q. Canada, pp. 771-782.
Määttänen, M., 1978. ON CONDITIONS FOR THE RISE OF SELF-EXCITED ICE INDUCED AUTONOMOUS OSCILLATIONS IN SLENDER MARINE PILE STRUCTURES. PhD Thesis, UNIVERSITY OF OULU.
Määttänen, M., 1982. True ice force by deconvolution, 1st International Modal Analysis Conference (IMAC), Orlando, FL, USA, pp. 556-590.
Määttänen, M., 1983. DYNAMIC ICE-STRUCTURE INTERACTION DURING CONTINOUS CRUSHING, U.S. Army Cold Regions Research and Engineering Laboratory, Hanover, NH 03755. CRREL Report 83-5.
Määttänen, M., Løset, S., Metrikine, A., Evers, K.-U., Hendrikse, H., Lønøy, C., Metrikin, I., Nord, T.S. and Sukhorukov, S., 2012. Novel ice induced vibration testing in a large-scale facility, "Ice Research for a Sustainable Environment"(IAHR), Dalian, China.
Määttänen, M., Marjavaara, P., Saarinen, S. and Laakso, M., 2011. Ice crushing tests with variable structural flexibility. Cold Regions Science and Technology, 67(3): 120-128.
Nord, T.S. and Määttänen, M., 2012. Modal analysis in ice structure interaction, IAHR, Dalian, China.
Nordström, L.J.L. and Nordberg, T.P., 2004. A time delay method to solve non-collocated input estimation problems. Mechanical Systems and Signal Processing, 18(6): 1469-1483.
Parloo, E., Verboven, P., Guillaume, P. and Van Overmeire, M., 2003. Force identification by means of in-operation modal models. Journal of Sound and Vibration, 262(1): 161-173.
Singh, S.K., Timco, G.W., Frederking, R. and Jordaan, I.J., 1990. TESTS OF ICE CRUSHING ON A FLEXIBLE STRUCTURE, OMAE Houston TX. USA, pp. 89-94.
Sodhi, D.S., 2001. Crushing failure during ice–structure interaction. Engineering Fracture Mechanics, 68(17–18): 1889-1921.
Takeuchi, T., Sakai, M., Akagawa, S. and Saeki, H., 2000. On the Factors Influencing the Scaling of Ice Forces, IUATAM Symposium on Scaling Laws in Ice Mechanics and Ice Dynamics, Fairbanks, USA, pp. 149-160.
Taylor, R., 2009. Analysis of Scale Effect in Compressive Ice Failure. PhD Thesis.
Timco, G. and Croasdale, K.R., 2006. HOW WELL CAN WE PREDICT ICE LOADS?, IAHR, Sapporo, Japan, pp. 167-174.
Timco, G.W., Frederking, R. and Singh, S.K., 1989. THE TRANSFER FUNCTION APPROACH FOR A STRUCTURE SUBJECTED TO ICE CRUSHING, POAC, Luleå, Sweden, pp. 420-430.
Wang, B.T., 2002. PREDICTION OF IMPACT AND HARMONIC FORCES ACTING ON ARBITRARY STRUCTURES: THEORETICAL FORMULATION. Mechanical Systems and Signal Processing, 16(6): 935-953.
Y.Toyama, T.Sensu, M.Minami and N.Yashima, 1983. Model tests on self-excited vibration on cylindrical structures, Port and Ocean Under Arctic conditions (POAC), Helsinki, pp. 834-844.